Ferroelectric PbTiO₃/SrRuO₃ Superlattices with Broken Inversion Symmetry

S. J. Callori,[1] J. Gabel,[1] D. Su,[2] J. Sinsheimer,[1] M. V. Fernandez-Serra,[1] and M. Dawber[1,*]

[1]*Department of Physics and Astronomy, Stony Brook University, Stony Brook, New York 11794-3800, USA*
[2]*Center for Functional Nanomaterials, Brookhaven National Laboratory, Upton, New York 11973-5000, USA*
(Received 13 January 2012; published 9 August 2012)

We have fabricated PbTiO₃/SrRuO₃ superlattices with ultrathin SrRuO₃ layers. Because of the superlattice geometry, the samples show a large anisotropy in their electrical resistivity, which can be controlled by changing the thickness of the PbTiO₃ layers. Therefore, along the ferroelectric direction, SrRuO₃ layers can act as dielectric, rather than metallic, elements. We show that, by reducing the concentration of PbTiO₃, an increasingly important effect of polarization asymmetry due to compositional inversion symmetry breaking occurs. The results are significant as they represent a new class of ferroelectric superlattices, with a rich and complex phase diagram. By expanding our set of materials we are able to introduce new behaviors that can only occur when one of the materials is not a perovskite titanate. Here, compositional inversion symmetry breaking in bicolor superlattices, due to the combined variation of *A* and *B* site ions within the superlattice, is demonstrated using a combination of experimental measurements and first principles density functional theory.

Artificially layered perovskite oxide superlattices provide many opportunities to develop systems with novel and tunable properties [1,2]. As far as ferroelectric superlattices are concerned, the insulating titanium perovskite oxides (e.g., PbTiO₃, BaTiO₃, CaTiO₃, and SrTiO₃) have to date been the most popular "building blocks." but the need for new functionalities, particularly related to magnetism, requires the use of a wider set of materials and a deep understanding of the new physical phenomenon related to interfaces. In this Letter an unconventional approach is demonstrated: we use a material that is normally metallic to play the role of a dielectric in a ferroelectric-dielectric superlattice.

The much-studied compound SrRuO₃ provides the proof of concept that metallic magnetic oxides can transform into thin-film dielectric components in certain heterostructures. In bulk, SrRuO₃ has the distorted perovskite orthorhombic *Pnma* structure, is metallic, and is ferromagnetic below $T_c = 160$ K [3–7]. It is also a commonly used electrode material for oxides, and the interface with ferroelectric oxides has been much studied [8–12]. However, SrRuO₃ becomes insulating in layers of thickness less than four unit cells (u.c.); this behavior has been observed in thin films [13–15] and in SrTiO₃/SrRuO₃ superlattices [16,17]. First principles investigations [18–20] and experiments [21–26] indicate that epitaxial strain, size effects, chemical pressure, surface reconstruction, and interaction with the substrate may all play an important role in the observed behavior. In a recent contribution, Verissimo-Alves *et al.* [27] showed from first principles calculations that a highly confined two-dimensional electron gas is formed at the interface in SrTiO₃/SrRuO₃ superlattices. We will show in this Letter that a similar effect occurs in PbTiO₃/SrRuO₃ superlattices, but that in the direction perpendicular to the interfaces PbTiO₃/SrRuO₃ superlattices containing single unit cell layers of SrRuO₃ are insulating and can be ferroelectric.

A second motivation for creating PbTiO₃/SrRuO₃ superlattices is that, as they have both *A* and *B* site variation, inversion symmetry can be compositionally broken [28,29]. As a result, an asymmetry is introduced in the ferroelectric double-well potential which can lead to "self-poling" materials. Self-poling ferroelectric materials are useful in piezoelectric applications where the desired mode of operation is to apply an electric field either with or against a fixed polarization direction to achieve, respectively, an expansion or contraction of the material. In a tricolor superlattice compositional breaking of inversion symmetry can occur with only *A* or *B* site variation. The effect has been seen with *A* site variation in trilayer superlattices containing BaTiO₃, CaTiO₃, and SrTiO₃ [30,31], and has been shown to be an appealing route towards magnetoelectric materials with tricolor variation on the *B* site [32,33], but until now this behavior has not been shown experimentally in bicolor superlattices.

Epitaxial growth of PbTiO₃/SrRuO₃ superlattices can be achieved on SrTiO₃ substrates as both PbTiO₃ and SrRuO₃ have in-plane lattice parameters close to that of SrTiO₃, which at room temperature is cubic with $a = 3.905$ Å. At room temperature bulk PbTiO₃ is tetragonal ($a = 3.904$ Å, $c = 4.15$ Å) and orthorhombic SrRuO₃ can be considered as pseudocubic with $a = 3.93$ Å. For this study, the $n/1$ PbTiO₃/SrRuO₃ [*n* unit cells PbTiO₃/ 1 unit cell SrRuO₃] superlattices were deposited using off-axis rf magnetron sputtering on (001) SrTiO₃ substrates, which had been treated with buffered HF and annealed to ensure TiO₂ termination. The SrRuO₃ layer thickness was grown to 1 u.c. for all the samples considered here, with the aim being that the SrRuO₃ layers should act as dielectrics, rather than metals. By contrast the thickness of the PbTiO₃ layer was changed from sample to sample, so that the relative effect of bulk ferroelectricity vs interfacially
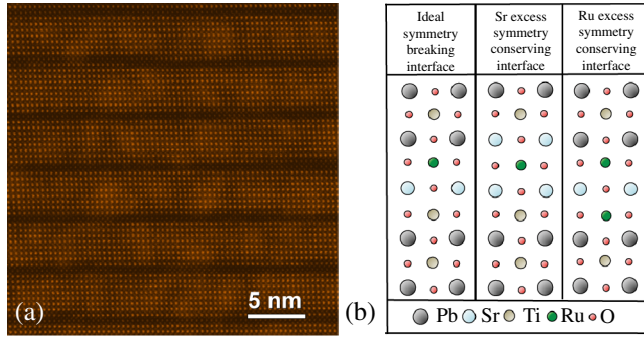
	Ideal symmetry breaking interface	Sr excess symmetry conserving interface	Ru excess symmetry conserving interface

FIG. 1 (color online). (a) A HR-STEM image of an 8/1 $PbTiO_3/SrRuO_3$ superlattice. (b) The three types of interfaces considered theoretically in this Letter, illustrated for the case of a 3/1 $PbTiO_3/SrRuO_3$ superlattice.

driven compositional inversion symmetry breaking could be assessed. The total number of bilayers in the superlattice was varied from one sample to another so that the total thickness of each sample was in each case as close as possible to 100 nm. Growth rates for the two materials within the superlattice were obtained from x-ray diffraction measurements performed on many preliminary samples. Bottom $SrRuO_3$ electrodes (20 nm in thickness) were deposited *in situ* for the samples used for electrical measurements, and gold top electrodes were added to the samples in a second deposition process. The superlattices were grown at a temperature of 550 °C and the $SrRuO_3$ electrodes were grown at 620 °C.

Experimentally, it has been demonstrated by Rjinders *et al.* [34] that when grown by pulsed laser deposition the termination of a $SrRuO_3$ film is affected by both deposition conditions and layer thickness, and that as a film grows on Ti terminated $SrTiO_3$ there is a conversion from a RuO_2 to a SrO termination layer. At a growth temperature of 700 °C this transition already occurs for a single unit cell $SrRuO_3$ layer, but at lower deposition temperatures, this transition occurs later in the growth, as the RuO_2 layer is comparably more stable at these conditions. As a consequence of the small thickness of our $SrRuO_3$ layers, the low deposition temperatures used in our process, and the different kinetic regime of sputtering as compared to pulsed laser deposition, a RuO_2 termination of our $SrRuO_3$ layers, may still be possible.

The epitaxial growth of our samples was confirmed by x-ray diffraction and high resolution (HR) scanning transmission electron microscopy (STEM). Figure 1(a) shows a HR STEM cross section of an 8/1 $PbTiO_3/SrRuO_3$ superlattice. The $PbTiO_3$ layers are the brightest because of the high atomic number of Pb, while the $SrRuO_3$ layers are less bright than $PbTiO_3$, but have enhanced brightness compared to $SrTiO_3$ (not shown) because the Ru ion has a higher atomic number than Ti. In addition to the STEM image shown, we also carried out STEM-EELS line scans [35], which support the ideality of our grown structures.

Although the interface most likely to form in $PbTiO_3/SrRuO_3$ superlattices if the atoms in the material are deposited in the same ratio as the parent targets breaks

inversion symmetry, it is possible to consider interfaces that might form which do not. In Fig. 1(b) we show three kinds of interfaces which we have studied using first principles calculations, which we illustrate for the case of a 3/1 superlattice. The ideal structure which breaks inversion symmetry is the first from the left in Fig. 1(b). In order to study the significance of the symmetry breaking effect, we also simulated two different kinds of interface which conserve symmetry: one in which one Pb-O plane has been replaced by a Sr-O plane, which is shown in the center of Fig. 1(b); and another (less likely due to the high volatility of Ru) unit cell in which a Ti-O plane has been replaced by a Ru-O plane, shown on the right.

We investigated the three kinds of interface shown above using first principles calculations. These were performed using density functional theory, using a basis of numerical atomic orbitals as implemented in the SIESTA code [36]. We used the same basis set and pseudopotentials as Verissimo-Alves *et al.* [27]. We studied the influence of spin polarization, the use of the generalized gradients approximation within the commonly used Wu-Cohen parametrization [37], and the effect of correlations within the LDA + U and LSDA + U approximations [38] which are the local density approximation and local spin density approximation, modified by the addition of a Hubbard U term. The different approximations used can affect the electronic properties of the metallic layer along the parallel direction. However, the electrical anisotropy is mostly dependent on the superlattice periodicity, and therefore results are computed using the local density approximation (LDA), which is the best method to characterize both the structural and electronic properties of the superlattices. Full details regarding the calculations can be found in the Supplemental Material [35]. We examined the electrical conductivity of the superlattices both in plane (σ_{xx}) and out of plane (σ_{zz}) by calculating the diagonal elements of the conductivity tensor within the relaxation time approximation to the Boltzmann transport equation [39]. The anisotropy in σ is fully determined by the anisotropy of the Fermi surface geometry, as determined by $\sigma_{\alpha\alpha} = -e^2\tau\sum_k v_{k\alpha}^2\delta(\epsilon_F - \epsilon_k)$. The relaxation time, τ, is the only variational parameter in the expression, and we choose $\tau = 1.3 \times 10^{-14}$ s after experimental results in bulk $SrRuO_3$ [40]. This approximation ignores the anisotropy of the electron-phonon scattering, although this is known to be a much smaller effect [39]. The results shown in Fig. 2(a) are for the ideal interfaces, but these quantities were also calculated for the two other cases and are qualitatively similar, again an indication that the anisotropy is almost fully determined by the inter-$SrRuO_3$ layer distance. We find, in agreement with Ref. [27], that the electrons in the single unit cell layers of $SrRuO_3$ are confined to that layer, so while the in-plane conductivity, σ_{xx}, of the structures does not change dramatically as the spacing between the layers is varied, the out-of-plane conductivity, σ_{zz}, decreases exponentially with a characteristic length of 1.3 Å as the thickness of the $PbTiO_3$ layers is increased.
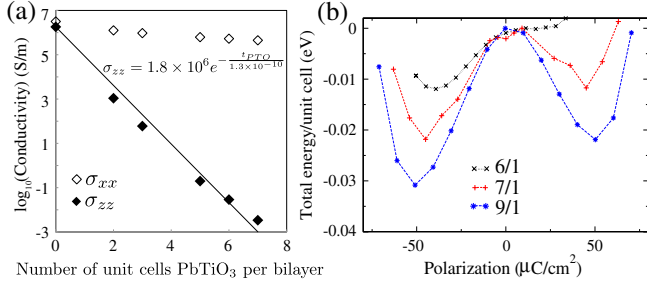
FIG. 2 (color online).   (a) Calculated conductivity both in plane and out of plane plotted a function of the number of unit cells of PbTiO$_3$ included in each bilayer (with zero corresponding with SrRuO$_3$ strained in plane to the SrTiO$_3$ lattice parameter). (b) Calculated total energy per unit cell as a function of polarization.
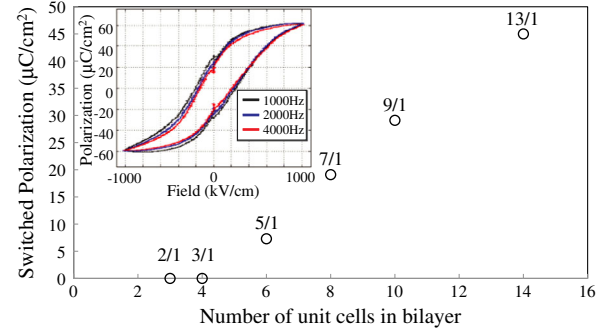

FIG. 3 (color online).   Switched polarization plotted as a function of the total number of unit cells in each bilayer. Inset: Polarization-field hysteresis loops measured at three different frequencies on a 7/1 sample.

In the two-component PbTiO$_3$/SrRuO$_3$ superlattices in which the inversion symmetry is broken by the ideal interface structure, our calculations predict a self-poling behavior. In Fig. 2(b) we show the energy of the superlattice as a function of the polarization. We computed the total energy of the system for atomic displacements along the line $\vec{r} = \vec{r}_{P_+} + u(\vec{r}_{P_-} - \vec{r}_{P_+})$, interpolating linearly between the two minima of the energy. These two minima are characterized by two different polarization states, P_{up} (higher energy minimum) and P_{down} (lower energy minimum). As shown in Table I, the simulations for the ideal interface show that, as the PbTiO$_3$ layer thickness is reduced, there is an increasingly large difference in the values of the stable up and down polarizations, until for the 5/1 superlattice, when the potential well has just one minimum, only the down polarization is stable.

The preference of one polarization state over another for superlattices with broken compositional inversion symmetry was seen in all of the calculation schemes used. In the spin polarized calculations for samples with single unit cell layers of SrRuO$_3$ the spin polarization is not affected by the direction of the polarization. However, in simulations of superlattices with symmetry breaking interfaces that have SrRuO$_3$ layers thicker than 1 u.c. the magnetization is different for the two polarization directions. Although it is not the focus of the present paper, this finding demonstrates the potential for the compositional breaking of inversion symmetry at the PbTiO$_3$/SrRuO$_3$ interface to enable a form of coupling between magnetism and ferroelectricity.

Experimental values for the switched ferroelectric polarization of the samples were obtained from polarization-electric field hysteresis loops performed on a number of samples. Polarization hysteresis was observed in samples with a PbTiO$_3$ layer thickness of 5 u.c. or greater. The experimentally measured polarization as a function of the total number of unit cells in each bilayer is shown in Fig. 3, along with characteristic loops measured at three different frequencies on the 7/1 sample shown as an inset. Successful hysteresis loops confirm that the thin layers of SrRuO$_3$ in the material are acting as dielectric layers, and allow a continuous polarization in the structure. An independent confirmation of ferroelectricity comes from x-ray diffraction reciprocal space maps around superlattice Bragg peaks, shown in the Supplemental Material [35]. These show diffuse scattering from the in-plane periodicity of stripe domains with polarization oriented up and down with respect to the substrate, and are similar to those seen in PbTiO$_3$/SrRuO$_3$ superlattices [41,42]. These domain features were observed in the 7/1, 9/1, and 13/1 superlattices, but not in the 5/1 superlattice. The lack of domain features in the 5/1 PbTiO$_3$/SrRuO$_3$ superlattice may be due to the relative instability of one polarization state with respect to each other, i.e., while the polarization can be switched under a field from one direction to the other, its equilibrium configuration is dominated by a single polarization direction. Direct comparisons between the calculated stable polarizations in the layer and the experimentally measured switched polarizations are difficult to make, as the two quantities,

TABLE I.   Calculated stable polarization magnitudes (DFT LDA) in the up and down directions for a selection of ideal superlattices.

| | Stable polarization (μC/cm^2) | | | |
| | Ideal | | Sr excess | Ru excess |
Superlattice	P_{down}	P_{up}	P	P
(PbTiO$_3$)$_5$(SrRuO$_3$)$_1$	35.8	unstable	2.0	23.3
(PbTiO$_3$)$_6$(SrRuO$_3$)$_1$	39.2	16.8	16.4	32.5
(PbTiO$_3$)$_7$(SrRuO$_3$)$_1$	45.0	45.1	27.2	44.2
(PbTiO$_3$)$_9$(SrRuO$_3$)$_1$	50.9	50.2	42.9	52.7

while related, are not identical. However, it can be seen that the polarization values and their dependence on the number of unit cells in each bilayer are qualitatively similar for the experiment and the three theoretical cases considered in Table I. For an equivalent composition the Ru excess super-lattices have higher polarizations than the Sr excess super-lattices. In the ideal case marked differences in the polarization value for the up and down state become notice-able for superlattices whose bilayers contain less than 7 u.c. of $PbTiO_3$. When the $PbTiO_3$ layer thickness is three layers or less the samples become fairly conductive in the out-of-plane direction, both in the theory and the experiment.

An indirect probe of the stable polarization is the average tetragonality (c/a) of ferroelectric superlattices, which can be measured using x-ray diffraction [43–45]. Our experimental measurements and first principles results from density functional theory (DFT) LDA calculations are shown in Fig. 4. As with the polarization values in Fig. 3, we have plotted the results in terms of the total number of unit cells per bilayer, and included for each set of values the nominal composition. However, the Sr and Ru excess struc-tures deviate from these ideal structures as described earlier; for the former one Pb-O plane has been replaced by a Sr-O plane, and for the latter a Ti-O plane has been replaced by a Ru-O plane. It is difficult to make a definite conclusion which interface is present in our experimental samples solely from comparing the experimental results with the theoretical predictions shown. However, we suggest that a comparison of the data over the whole range of the plot would tend to exclude the Sr excess interface, and although the Ru excess interface matches the experimental data relatively well, this interface is unlikely to occur in the experiment due to the high volatility of Ru. An interesting point in this figure is that the average tetragonality begins to increase again as the number of unit cells in each bilayer is decreased. This is because, in contrast to $PbTiO_3/SrTiO_3$ where $SrTiO_3$ grown on $SrTiO_3$ has a tetragonality of 1 and the c/a montonically decreases, as the amount of $PbTiO_3$ decreases, $SrRuO_3$ grown on

$SrTiO_3$ has a tetragonality of 1.03. It appears that the c axis lattice parameter of paraelectric $PbTiO_3$ in these superlattices is quite low, both in experiment and theory and is certainly well below the value of approximately 1.03 that is predicted by the Landau theory [44]. The upturn in the c/a value occurs for the Ru excess samples first as these are, for each sample, essentially half a unit cell closer to being $SrRuO_3$ than the corresponding ideal superlattice.

The effect that the compositional breaking of inversion symmetry has on functional properties is most evident in the dielectric response of the samples. In Fig. 5, we show the dielectric constant measured as a function of electric field (at a frequency of 10 kHz). The measurements show an evolution from a typical butterfly loop for $PbTiO_3$ rich samples (13/1 and 9/1 samples) to a highly asymmetric curve with a greatly enhanced peak dielectric constant for the 3/1 sample. An unusual characteristic where two peaks are seen on each voltage trace is displayed in the 5/1 sample. The composition at which the transition from conventional ferroelectric behavior occurs (approximately 7/1) matches the composition highlighted by theory at which compositional inversion symmetry breaking becomes a dominant factor. To summarize our picture of this system, the 3/1 sample can be characterized as a spontaneously polarized nonswitchable insulator (or, in other words, an interfacially driven pyroelectric). Samples between 7/1 and 3/1 are best described as asymmetric ferroelectrics. Samples with $PbTiO_3$ layers thicker than 7 u.c., while still containing interfaces which compositionally break inversion symmetry, are not greatly affected by them.

Besides the direct results presented here, our study offers a general demonstration of the possibilities unlocked by expanding the material set used in ferroelectric superlattices. Our findings should motivate a broader exploration of candidate materials for the development of new artificially layered ferroelectrics. In particular, besides the self-poling behavior that compositional broken inversion symmetry produces, the use of thin metallic materials as dielectric layers has intriguing potential for the development of highly coupled multiferroics.

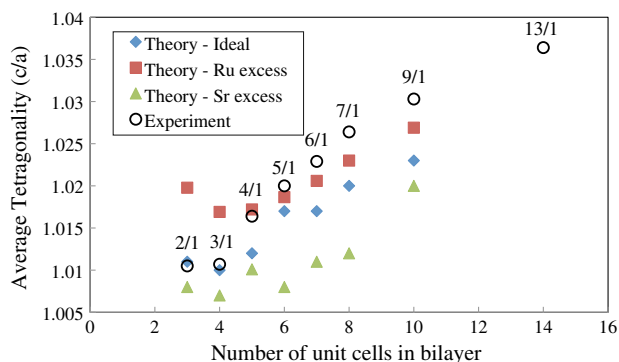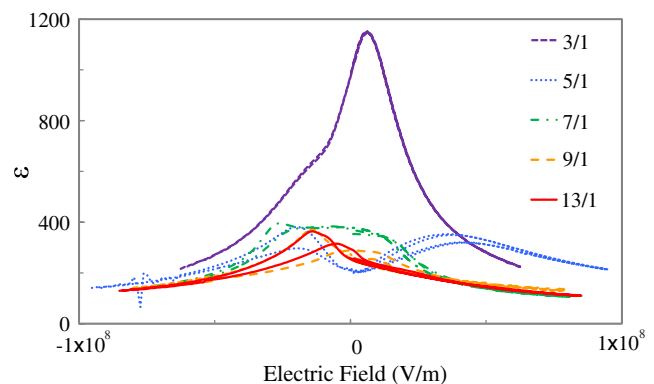

FIG. 4 (color online).   Average tetragonality, or the ratio of the average out-of-plane lattice parameter c to the lattice parameter of the $SrTiO_3$ substrate a, (i.e., c/a), plotted as a function of the total number of unit cells in each bilayer. As well as the experimental results, results from DFT LDA calculations for three different kinds of interfaces are shown.

FIG. 5 (color online).   Dielectric constant-field loops for five of our samples.

*matthew.dawber@stonybrook.edu

[1] M. Dawber, N. Stucki, C. Lichtensteiger, S. Gariglio, and J.-M. Triscone, J. Phys. Condens. Matter **20**, 264015 (2008).

[2] P. Zubko, S. Gariglio, M. Gabay, P. Ghosez, and J.-M. Triscone, Annu. Rev. Condens. Matter Phys. **2**, 141 (2011).

[3] P. B. Allen, H. Berger, O. Chauvet, L. Forro, T. Jarlborg, A. Junod, B. Revaz, and G. Santi, Phys. Rev. B **53**, 4393 (1996).

[4] D. J. Singh, J. Appl. Phys. **79**, 4818 (1996).

[5] I. I. Mazin and D. J. Singh, Phys. Rev. B **56**, 2556 (1997).

[6] J. S. Dodge, C. P. Weber, J. Corson, J. Orenstein, Z. Schlesinger, J. W. Reiner, and M. R. Beasley, Phys. Rev. Lett. **85**, 4932 (2000).

[7] L. Capogna, A. P. Mackenzie, R. S. Perry, S. A. Grigera, L. M. Galvin, P. Raychaudhuri, A. J. Schofield, C. S. Alexander, G. Cao, S. R. Julian, and Y. Maeno, Phys. Rev. Lett. **88**, 076602 (2002).

[8] J. Junquera and P. Ghosez, Nature (London) **422**, 506 (2003).

[9] G. Gerra, A. K. Tagantsev, N. Setter, and K. Parlinski, Phys. Rev. Lett. **96**, 107603 (2006).

[10] M. Stengel and N. A. Spaldin, Nature (London) **443**, 679 (2006).

[11] P. Aguado-Puente and J. Junquera, Phys. Rev. Lett. **100**, 177601 (2008).

[12] J. Shin, A. Borisevich, V. Meunier, J. Zhou, E. W. Plummer, S. V. Kalinin, and A. P. Baddorf, ACS Nano **4**, 4190 (2010).

[13] D. Toyota, I. Ohkubo, H. Kumigashira, M. Oshima, T. Ohnishi, M. Lippmaa, M. Kawasaki, and H. Koinuma, Appl. Phys. Lett. **87**, 162508 (2005); J. Appl. Phys. **99**, 08N505 (2006).

[14] M. Schultz, S. Levy, J. W. Reiner, and L. Klein, Phys. Rev. B **79**, 125444 (2009).

[15] J. Xia, W. Siemons, G. Koster, M. R. Beasley, and A. Kapitulnik, Phys. Rev. B **79**, 140407(R) (2009).

[16] M. Izumi, K. Nakazawa, and Y. Bando, J. Phys. Soc. Jpn. **67**, 651 (1998).

[17] H. Kumigashira, M. Minohara, M. Takizawa, A. Fujimori, D. Toyota, I. Ohkubo, M. Oshima, M. Lippmaa, and M. Kawasaki, Appl. Phys. Lett. **92**, 122105 (2008).

[18] A. T. Zayak, X. Huang, J. B. Neaton, and K. M. Rabe, Phys. Rev. B **74**, 094104 (2006); **77**, 214410 (2008).

[19] J. M. Rondinelli, N. M. Caffrey, S. Sanvito, and N. A. Spaldin, Phys. Rev. B **78**, 155107 (2008).

[20] P. Mahadevan, F. Aryasetiawan, A. Janotti, and T. Sasaki, Phys. Rev. B **80**, 035106 (2009).

[21] G. Herranz, B. Martinez, J. Fontcuberta, F. Sanchez, C. Ferrater, M. V. Garcia-Cuenca, and M Varela, Phys. Rev. B **67**, 174423 (2003).

[22] K. W. Kim, J. S. Lee, T. W. Noh, S. R. Lee, and K. Char, Phys. Rev. B **71**, 125104 (2005).

[23] R. G. Moore, Jiandi Zhang, V. B. Nascimento, R. Jin, Jiandong Guo, G. T. Wang, Z. Fang, D. Mandrus, and E. W. Plummer, Science **318**, 615 (2007).

[24] A. Grutter, F. Wong, E. Arenholz, M. Liberati, and Y. Sukuki, J. Appl. Phys. **107**, 09E138 (2010).

[25] M. Ziese, I. Vrejoiu, and D. Hesse, Phys. Rev. B **81**, 184418 (2010).

[26] K. J. Choi, S. H. Baek, H. W. Jang, L. J. Belenky, M. Lyubchenko, and C.-B. Eom, Adv. Mater. **22**, 759 (2010).

[27] M. Verissimo-Alves, P. Garcia-Fernandez, D. I. Bilc, P. Ghosez, and J. Junquera, Phys. Rev. Lett. **108**, 107003 (2012).

[28] N. Sai, B. Meyer, and D. Vanderbilt, Phys. Rev. Lett. **84**, 5636 (2000).

[29] N. Sai, B. Meyer, and D. Vanderbilt, *Fundamental Physics of Ferroelectrics* (AIP, Melville, NY, 2001), p. 218.

[30] M. P. Warusawithana, E. V. Colla, J. N. Eckstein, and M. B. Weissman, Phys. Rev. Lett. **90**, 036802 (2003).

[31] H. N. Lee, H. M. Christen, M. F. Chisholm, C. M. Rouleau, and D. H. Lowndes, Nature (London) **433**, 395 (2005).

[32] A. J. Hatt and N. A. Spaldin, Appl. Phys. Lett. **90**, 242916 (2007).

[33] H. Yamada, H. Sato, H. Akoh, N. Kida, T. Arima, M. Kawasaki, and Y. Tokura, Appl. Phys. Lett. **92**, 062508 (2008).

[34] G. Rijnders, D. H. A. Blank, J. Choi, and C. B. Eom, Appl. Phys. Lett. **84**, 505 (2004).

[35] See Supplemental Material at http://link.aps.org/supplemental/10.1103/PhysRevLett.109.067601 for STEM-EELS line scans, full details of first principles calculations, and x-ray reciprocal space maps for selected samples.

[36] J. M. Soler, E. Artacho, J. D. Gale, A. García, J. Junquera, P. Ordejón, and D. Sánchez-Portal, J. Phys. Condens. Matter **14**, 2745 (2002).

[37] Z. Wu and R. E. Cohen, Phys. Rev. B **73**, 235116 (2006).

[38] M. Wierzbowska, D. Sanchez-Portal, and S. Sanvito, Phys. Rev. B **70**, 235209 (2004).

[39] P. B. Allen, W. E. Pickett, and H. Krakauer, Phys. Rev. B **37**, 7482 (1988).

[40] G. Santi and T. Jarlborg, J. Phys. Condens. Matter **9**, 9563 (1997).

[41] P. Zubko, N. Stucki, C. Lichtensteiger, and J.-M. Triscone, Phys. Rev. Lett. **104**, 187601 (2010).

[42] J. Y. Jo, P. Chen, R. J. Sichel, S. J. Callori, J. Sinsheimer, E. M. Dufresne, M. Dawber, and P. G. Evans, Phys. Rev. Lett. **107**, 055501 (2011).

[43] M. Dawber, C. Lichtensteiger, M. Cantoni, M. Veithen, P. Ghosez, K. Johnston, K. M. Rabe, and J.-M. Triscone, Phys. Rev. Lett. **95**, 177601 (2005).

[44] M. Dawber, N. Stucki, C. Lichtensteiger, S. Gariglio, P. Ghosez, and J.-M. Triscone, Adv. Mater. **19**, 4153 (2007).

[45] E. Bousquet, M. Dawber, N. Stucki, C. Lichtensteiger, P. Hermet, S. Gariglio, J.-M. Triscone, and P. Ghosez, Nature (London) **452**, 732 (2008).